arXiv:cond-mat/0211501v1 [cond-mat.soft] 22 Nov 2002

Pore Stability and Dynamics in Polymer Membranes

H. Bermudez,[1, *] H. Aranda-Espinoza,[2] D. A. Hammer,[1, 2] and D. E. Discher[1, 2]
[1]*Department of Chemical and Biomolecular Engineering,*
University of Pennsylvania, Philadelphia, Pennsylvania 19104
[2]*Institute for Medicine and Engineering, University of Pennsylvania, Philadelphia, Pennsylvania 19104*

Vesicles self-assembled from amphiphilic diblock copolymers exhibit a wide diversity of behavior upon electroporation, due to competitions between edge, surface and bending energies that drive the system, while different viscous dissipation mechanisms determine the timescales. These effects are manifestations of the varying membrane thickness d from what are essentially chemically identical molecules. For smaller d, we find large unstable pores and the resulting membrane fragments reassemble into vesicles within minutes. Vesicles with larger d form long-lived pores of nanometer dimension that could be potentially useful for sieving applications and drug delivery.

PACS numbers: 82.70.Uv, 68.65.-k, 87.68.+z

Membranes are ubiquitous in biology and play a central role in the distribution of macromolecules both inside and outside cells. Additionally, specialized transmembrane machinery serves to exquisitely regulate intracellular concentrations at their optimal, non-equilibrium conditions [1]. These transmembrane gradients are known to be involved in signaling and other regulatory processes. Thus the control and exploitation of biomembrane selectivity has been and continues to be the focus of intense research [2]. One approach to manipulate biomembranes is known as electroporation, where an electric field is used to transiently disrupt the membrane [3]. In the brief time the membrane is open, solutes or macromolecules can diffuse into or out of the cell. Technological applications for DNA delivery and creation of hybrid cells have employed electroporation, although cell viability is not always preserved [3].

Necessarily generated during biological processes are transmembrane potentials V_m and membrane tensions τ, as a result of electrostatic or mechanical forces. The continuing obstacle to approaching biological systems is that their complexity can obscure underlying physical mechanisms. Taking a reductionist approach, we have chosen to use synthetic vesicles formed from diblock copolymers, called polymersomes. These self-assembling diblocks are amphiphilic, with the hydrophilic portion being poly(ethylene oxide) (PEO) and the hydrophobic part composed of either polybutadiene (PBD) or its saturated form, poly(ethylethylene) (PEE) [4]. The synthetic basis allows for creation of a family of varying molecular weight $\bar{M}_n$ from $\approx 4-20$ kg/mol [5]. The resulting hydrophobic thickness d ranges from $8-21$ nm, compared to biomembranes of $3-5$ nm. Systematic investigations of electroporation are therefore motivated from both a biological and a physical perspective. In this Letter, we report our observations of a wide diversity of pore behavior, owing to the expanded range of d that is available with polymeric systems.

The experimental procedure closely follows Aranda-Espinoza, *et al.* [6]. In all cases, we used the film rehydration method to prepare vesicles, as is common for liposomes. A combination of phase contrast and fluorescence microscopy were used to monitor any changes in vesicle integrity that occured following pore formation [7].

The energetics of a circular hole of size r in a flat, infinitely thin, membrane can be most simply described by $E = 2\pi r\Gamma - \pi r^2\Sigma$, where Γ and Σ are the line and surface tensions of the membrane, respectively [8]. The line tension accounts for the energetic penalty involved with having a hole and the surface tension reflects the energy associated with a loss of membrane area. This relation predicts a metastable pore size $r^* = \Gamma/\Sigma$ obtained from $dE/dr = 0$. Pores of size $r < r^*$ will reseal and those with $r > r^*$ will grow without bound.

More complex models of pore growth include a dynamic surface tension, predicting a stable pore size [9, 10], but our observations indicate unstable pores in almost every case for **OE7** ($d = 8$ nm) and **OB16** ($d = 11$ nm), indicating a *small* value of Γ relative to the surface tension Σ. However, we need to consider the influence of membrane thickness on both Γ and Σ. At the moment of poration, Σ is the lysis tension Σ_c, and previous work has shown that $\Sigma_c \sim d$ [6]. The dependence of Γ on d, considering both hydrophobic and hydrophilic pores, leads to the same scaling of $\Gamma \sim d$. For a hydrophobic pore, the line tension is most simply the product of the exposed length d and the interfacial energy density γ: $\Gamma \sim \gamma d$. For a hydrophilic pore, Γ should scale as the bending modulus k_c multiplied by the curavture $\sim 2/d$. Simple elastic models predict $k_c \sim d^2$ [11] and hence $\Gamma \sim d$ again.

We therefore have the counterintuitive result that the metastable pore size does not depend on membrane thickness. We do indeed see large pores from **OE7** to **OB16** but **OB18** ($d = 15$ nm) and **OB19** ($d = 21$ nm) exhibit significantly smaller, and long-lived, pores. This abrupt change is presumed to be a result of increasing viscosity or chain entanglements within the hydrophobic region of the membrane [5, 12]. The lifetime of pores is largely dictated by the dynamics of the membrane. Liposomes are known to reseal quickly, with a few notable exceptions [13]. Under no external stresses, viscous dissipation at the interface and within the membrane are the obstacles to in-plane material rearrangement.

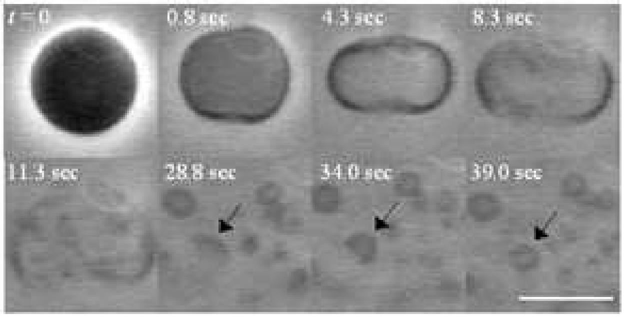

Figure 1: Time sequences of an **OE7** ($d = 8$ nm) vesicle following electroporation. The first reassembled vesicle appears at $t \approx 26$ sec, indicative of a large edge energy compared to the bending energy. The arrows indicate a particular disk reassembling. Scale bar is 10 μm.

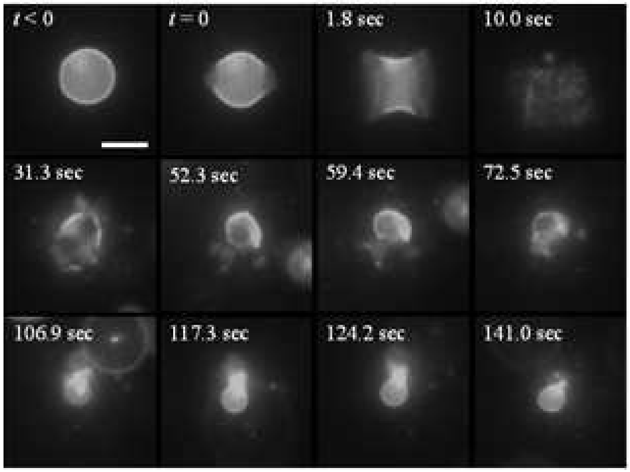

Figure 2: Time sequences of **OB16** ($d = 11$ nm) following poration are visualized with fluorescently labeled membranes. Vesicle reassembles at $t \approx 110$ sec. Note disk-like intermediates with rough edges. Scale bar is 10 μm.

For large pores (> 1 μm) such as those in **OE7** and **OB16**, we can visualize $r(t)$ by optical microscopy. Although both **OE7** and **OB16** exhibit unstable pores, they both reassemble rather quickly (Fig. 1). To our knowledge this is the first direct visualization of vesicle reassembly. Prior work has been focused in the suboptical regime and timescales for assembly have been of order minutes [14]. This closure reflects the relative large magnitude of the edge energy (line tension) compared to the bending energy, characterized by a "vesiculation index" $V_f \sim \Gamma R_d / k_c$ [15], where R_d is the radius of a disk and k_c the bending modulus. By assuming an attempt frequency $1/\tau_z$ based on viscous drag in the solution [16], we can calculate for **OE7**, $V_f = 2\left[1 - \sqrt{k_b T \ln(\tau_a/\tau_z)/8\pi k_c}\right] \approx 1.92$. This reflects the rapid transition of **OE7** into vesicles (*i.e.*, small reassembly time τ_a) from what are presumably disk-like or cylindrical micelles.

Membranes of **OB16** reassemble over a few minutes, indicating a smaller value of V_f compared to **OE7**. Visualization of the **OB16** process was possible only with fluorescently labeled membranes, as the fragments drift substantially before reassembling. Initially, membrane is clearly lost as the pores grow to several microns in diameter (Fig. 2), again suggestive of a small line tension relative to the surface tension. The hydrophobic dye indicates that **OB16** has an increased preference to form cylindrical or disk-like aggregates upon loss of membrane integrity (Fig. 2). This is consistent with observations that morphological boundaries (*e.g.*, lamellar-to-cylindrical) shift toward lower hydrophilic block fraction with increasing $\bar{M}_n$ [17], as well as with the longer reassembly time. **OE7** and **OB16** have characteristic reassembly times τ_a that are 20 and 100 sec, respectively. From scaling arguments [16], one can show that $\tau_a \sim \exp(d^2)$, indicating that even if a larger copolymer such as **OB19** were able to reassemble, the timescale would be several hours. Previous investigations of egg lecithin vesicle reassembly could not be visualized due to the rapid transition from disks to vesicles [18]. Only with the addition of an "edge-active" agent could disks be made sufficiently metastable for observation via electron microscopy. These findings are not surprising given that using the scaling relation above and taking $d = 3$ nm for a lecithin bilayer would correspond to τ_a of only a few seconds.

By extending the analysis of hole growth in thin polymer films [19], several groups have developed a framework for describing pore growth in cells and artificial vesicles [9, 10]. There is an initial, viscous dissipation within the membrane which at a later time crosses over to a regime dominated by dissipation in the surrounding fluid. For **OB16** (Fig. 3a), the only system we can unambiguously observe, we find that the pore growth process is almost entirely described by viscous losses within the membrane. The time constant for the initial regime τ_1 (0.67 ± 0.05 sec) allows us to determine the membrane viscosity $\eta_m = \tau_1 \Sigma / d \approx 10^6$ Pa sec. The resulting viscosity is three orders of magnitude larger than typical lipid membrane viscosities calculated by pore growth analysis ($\eta_m \approx 10^3$ Pa sec [10]), consistent with findings by other groups using different techniques [20]. In the limit where the dissipation is primarily due to the surrounding fluid viscosity η_i, pores will grow at a constant velocity [21]. From Fig. 3b, this is clearly not the case. We can also calculate the crossover radius r_c to the inertial regime as $\eta_m d / \eta_i \sim 10$ meters – indicating that this second regime is never reached for our micron-size vesicles.

The small pores (< 1 μm) in **OB18** and **OB19** re-

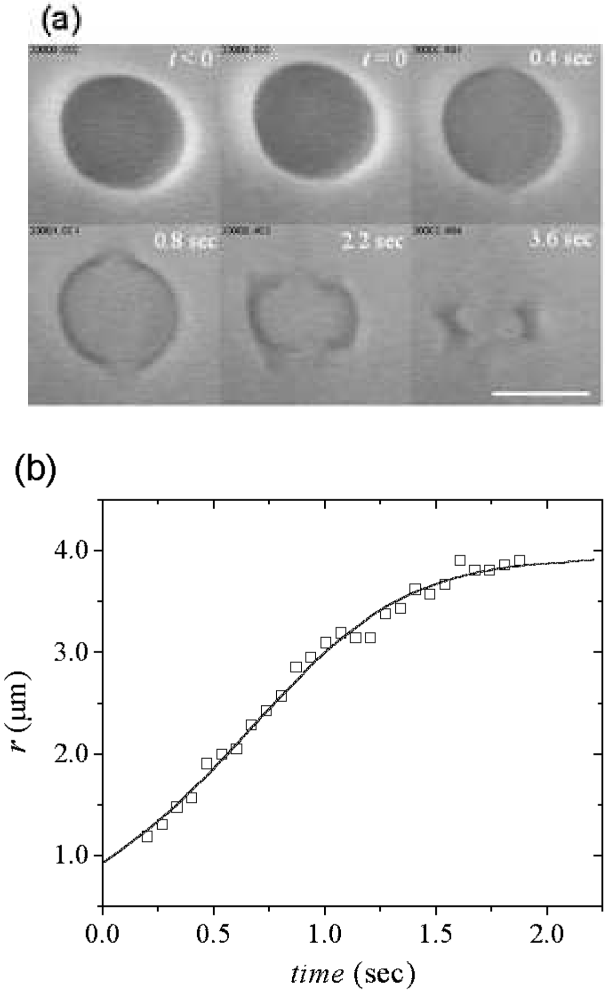

Figure 3: (a) Phase constrast imaging and (b) corresponding plot of pore radius r growth with time for **OB16**. The line is a theoretical fit that is dominated by viscous losses within the membrane. The resulting time constant τ_1 is 0.67 ± 0.05 sec ($N = 6$). The error in measuring r is $\pm 0.5\,\mu$m, limited by optical resolution. Scale bar is 10 μm

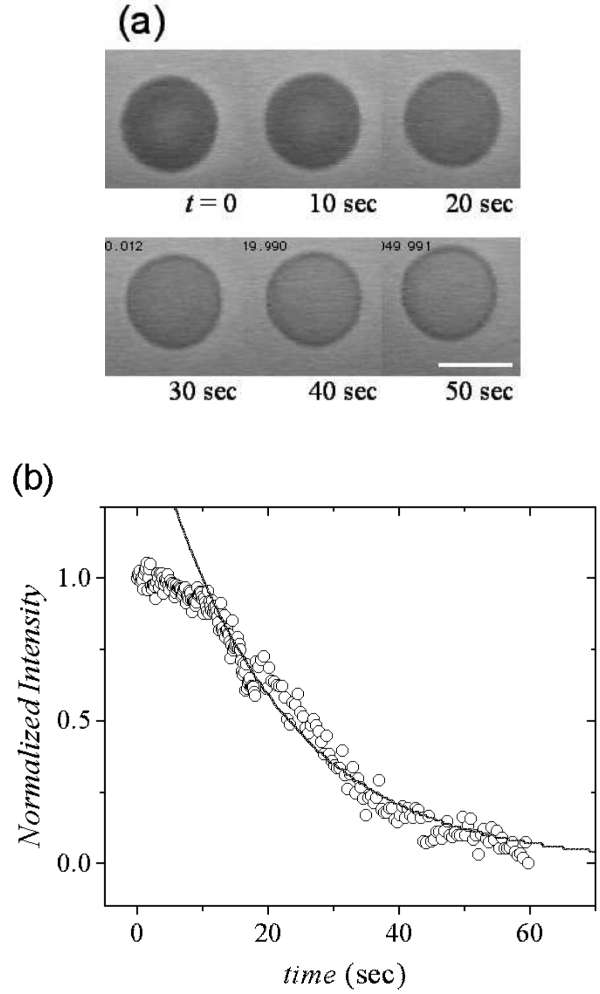

Figure 4: (a) Loss of phase contrast in **OB19** ($d = 21$ nm) due to escape of sucrose. (b) Corresponding normalized intensity of encapsulated sucrose versus time. Solid line is a fit to diffusion through a porous membrane, giving an effective permeability $\omega = 0.10 \pm 0.03$ μm/sec ($N = 3$). Scale bar is 10 μm.

quire a slightly different analysis. In this case, the intensity of encapsulant $I(t)$ is monitored, as pores cannot be directly observed (Fig. 4a). For a vesicle of size R_v, there is an initial "leak-out" regime, where solute loss is driven by Laplace pressure $\Delta P = 2\Sigma/R_v$, lasting several milliseconds for nanometer-size pores. We cannot observe this regime, but the tension will relax on this timescale $\tau_k \sim \eta_i R_v^2/r\Sigma$, and is followed by diffusion of solute through pores [10]. By fitting our data (Fig. 4b) to a simple exponential decay model of transport through porous membranes [22], we can obtain a time constant $\tau_d = R_v/3\omega$, where ω is the effective membrane permeability. There is an initial time lag in the intensity decay $t_{lag} \approx 10$ sec, which we tentatively attribute to hindered release of solute due to the PEO chains lining the nascent pores. The time constant increases with membrane thickness ($\tau_d = 13 \pm 4$ sec for **OB18** and $\tau_d = 17 \pm 6$ sec for **OB19**), reflecting either slower dynamics within the membrane and/or smaller pore sizes. The net result is an effective (sucrose) permeability $\omega = 0.22 \pm 0.15$ μm/sec for **OB18** and $\omega = 0.10 \pm 0.03$ μm/sec for **OB19**.

To estimate the size of sub-micron pores, we encapsulated fluorescent dextrans of various molecular weights and subjected these vesicles to electroporation (Fig. 5). Sucrose, which can be viewed under phase contrast and has a size ≈ 0.6 nm, always escapes the porated membrane. The FITC-labeled dextran of $\bar{M}_n \approx 4.4$ kg/mol and a TRITC-labeled dextran of $\bar{M}_n \approx 160$ kg/mol were retained over approximately 10 minutes. The sizes of these dextrans can be estimated by scaling relations [22]

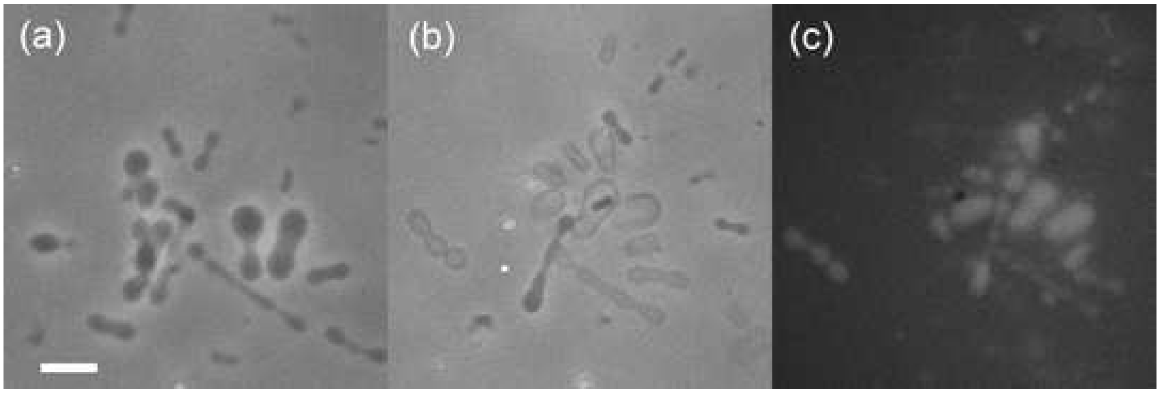

Figure 5: **OB18** electroporation and encapsulant retention. (a) $t < 0$, sucrose appears dark under phase contrast microscopy. (b) At $t = 1.2$ min, phase contrast indicates that sucrose has escaped, while (c) fluorescence shows that TRITC-dextran (160 kg/mol) is still retained. Scale bar is 25 μm.

to give hydrodynamic radii of $R_h \approx 2$ nm and $R_h \approx 5$ nm for the FITC and TRITC-dextrans, respectively. Thus although the pore size is only a few nanometers, given the dextran polydispersity (≈ 1.5), more precise measurements on the pore size will be published elsewhere [23].

In summary, we have observed for the first time vesicle formation from disk-like fragments, allowing us to obtain scaling relations for reassembly time. In certain cases, the slow dynamics of pore growth can be used to obtain the membrane viscosity (*e.g.*, **OB16** $\eta_m = 10^6$ Pa sec), qualitatively consistent with observations by other groups [20]. Sucrose leakage from thicker membranes (**OB18** and **OB19**) gives effective membrane permeabilities of vesicles with nanometer-scale pores. Control of the size and number of these pores by methods such as crosslinking [24] invites speculation on possible applications such as controlled drug delivery as well as for experimental tests of predictions for (bio)polymer translocation through pores [25, 26]. The results illustrate the rich diversity of behavior possible by changing a critical length scale d, with other chemistries potentially providing even more distinctive effects.

Funding was provided NSF-MRSEC's at Penn and the University of Minnesota, and NASA. The authors thank P. Photos for stimulating discussions.

---

[*] Electronic address: bermudez@seas.upenn.edu

[1] B. Alberts, *et al.*, *Essential Cell Biology* (Garland, New York, 1997).
[2] P. Barton, *et al.*, Angew. Chem. Int. Ed. **41**, 3878 (2002).
[3] E. Neumann, *et al.*, *Electroporation and Electrofusion in Cell Biology* (Plenum, New York, 1989).
[4] M.A. Hillmyer and F.S. Bates, Macromolecules **29**, 6994 (1996).
[5] H. Bermudez, *et al.*, Macromolecules **35**, 8203 (2002).
[6] H. Aranda-Espinoza, *et al.*, Phys. Rev. Lett. **87**, 208301 (2001).
[7] We used 0.3 M sucrose as our rehydrating solution, with vesicles later suspended in an osmotically-matched glucose solution, thus settling to the bottom of the chamber. The density difference coincides with a refractive index difference, allowing the use of phase contrast microscopy. Fluorescent labeling of the membrane is accomplished by incorporation of a hydrophobic dye (PKH26, Sigma) into the bilayer, which permits visualization of any membrane fragments or cylindrical micelles that might be present.
[8] J.D. Litster, Phys. Lett. **53A**, 193 (1974); B.V. Derjaguin and Yu.V. Gutop, Kolloid Zh. **24**, 431 (1962).
[9] H. Isambert, Phys. Rev. Lett. **80**, 3404 (1998)
[10] O. Sandre, L. Moreaux, F. Brochard-Wyart, Proc. Natl. Acad. Sci. USA **96**, 10591 (1999); F. Brochard-Wyart, P. G. de Gennes, O. Sandre, Physica A **278**, 32 (2000).
[11] M. Bloom, E. Evans, O.G. Mouritsen, Q. Rev. Biophys. **24**, 293 (1991).
[12] J.C-M. Lee, *et al.*, Macromolecules **35**, 323 (2002).
[13] D. Zhelev and D. Needham, Biochim. Biophys. Acta **1147**, 89 (1993). J.D. Moroz and P. Nelson, Biophys. J. **72**, 2211 (1997).
[14] Y. Xia, *et al.*, Langmuir **18**, 3822 (2002).
[15] P. Fromherz, Chem. Phys. Lett. **94**, 259 (1983).
[16] J. Leng, S.U. Engelhaaf, M.E. Cates, Europhys. Lett. **59**, 311 (2002).
[17] Y-Y. Won, *et al.*, J. Phys. Chem. B **106**, 3354 (2002).
[18] P. Fromherz and D. Rüppel, FEBS Lett. **179**, 155 (1985).
[19] G. Debrégeas, P. Martin, F. Brochard-Wyart, Phys. Rev. Lett. **75**, 3886 (1995).
[20] R. Dimova, *et al.*, Eur. Phys. J. E **7**, 241 (2002).
[21] J.F. Joanny and P.G. de Gennes, Physica A **147**, 238 (1987).
[22] R.K. Hobbie, *Intermediate Physics for Medicine and Biology.* (Springer-Verlag, New York, 1997).
[23] H. Bermudez, *et al.* (unpublished).
[24] B. Discher, *et al.*, J. Phys. Chem. B **106**, 2848 (2002).
[25] S.E. Hendrickson, *et al.*, Phys. Rev. Lett. **85**, 3057 (2000); A. Meller, L. Nivon, D. Branton, Phys. Rev. Lett. **86**, 3435 (2001).
[26] M. Muthukumar, Phys. Rev. Lett. **86**, 3188 (2001); D.K. Lubensky and D.R. Nelson, Biophys. J. **77**, 1824 (1999).